MICROSTRUCTURAL AND MICROMECHANICAL CHARACTERIZATION OF A DUPLEX MULTILAYER COATED H13 TOOL STEEL[1]

Abel André Cândido Recco[2]
André Paulo Tschiptschin[3]

Abstract

Quenched and tempered H13 tool steel was plasma nitrided and PVD coated in a hybrid reactor aiming to obtain a TiN/TiC multi-layer coating deposited on a plasma nitrided substrate, with a more gentle transition of elastic-plastic properties between the outermost layer of the coating and the substrate. Duplex treatment (plasma nitriding and PVD coating) was carried out in a hybrid reactor. Plasma nitriding preceded the DC triode magnetron sputtering PVD process, conducted inside the same chamber, using CH_4 and N_2 as reactive gases. Multi-layer TiN/TiC coatings deposited on a nitrided H13 substrate were obtained. Deposited TiC layers were characterized as containing 18.4 at% and 32.3 at% C, in a cF8 NaCl type unit cell, respectively. The TiN layer showed 41.9 at% N, also in a cF8 NaCl type unit cell. The multi-layer coating showed a gentle transition of elastic-plastic properties assessed by the H/E* and the H^3/E^{*2} ratios and the elastic recovery as a function of the distance from the surface of the specimen. The adhesion of the multi-layered coating to the substrate was greater in the case of the duplex coated specimen compared to the non duplex treated H13 steel.

Keywords: PVD-TiN; PVD-TiC; Plasma nitriding; PVD coating; Multilayer coatings.

INTRODUCTION

The mechanical systems being designed nowadays operate in ever more severe conditions, sustaining high applied loads, higher temperatures, greater sliding speeds and much more severe environments. The combination of usually conflicting properties is required in order to achieve higher productivity, high power efficiency, low energy consumption and low levels of emissions. The design of these mechanical systems involve the combination of properties such as low friction, high wear resistance, high load bearing capacity and fatigue resistance.

When subjected to high intensity loading, a thin coating may collapse, mainly due to substrate elastic and plastic deformation, resulting in the premature failure of the coating. For many applications the performance of a coating is limited by the mechanical properties of the substrate material itself. Thin films require a mechanical support given by the substrate material to avoid the so-called 'eggshell effect', granting good adhesion to the hard coating.

Optimization of tribological properties of materials comprises designing coating systems with different architectures, defined by a sequence of deposited coating layers that should resist to physical, physical-chemical and mechanical interactions arisen in service.

Different types of coating structures may be found in today's coating technology: single layer coatings, sandwich coatings and graded coatings. Most commercial CVD and PVD coatings are made up of one single layer often containing one structure phase. Among the most frequent are TiC, TiN, CrN, alumina (Al_2O_3) and diamond like carbon (DLC). They are usually applied directly onto the surface of a homogeneous substrate material. Sometimes the monolayer may be constituted by more than one component or by a gradient of compositions with mechanical properties varying accordingly.

Duplex coatings, on the other side, are obtained by combining a surface treatment of the substrate with a coating deposition. Single layer and multilayer coatings can be applied over pre-nitrided or any other diffusion treated surface.

The aim of this work is to characterize the microstructure and mechanical properties of a multilayered coating deposited on the surface of a plasma nitrided H13 tool steel.

EXPERIMENTAL

Quenched and tempered H13 mold tool steel specimens were duplex treated in a hybrid Triode Magnetron Sputtering (TMS) reactor. Plasma nitriding and PVD coating were done inside the same chamber, by changing the processing parameters used for each of the diffusion and coating treatments steps. When duplex treatments are performed in a hybrid reactor, contact of the specimen´s surface with air, between the treatments, is avoided and no cleaning or activating of the pre-nitrided surface is needed. Plasma Nitriding was carried out in conditions where no white layer can be formed. After Plasma Nitriding, PVD coating is carried out, by depositing, at first, a Ti interlayer to grant adhesion of the TiC and TiN layers. After deposition of the Ti interlayer reactive deposition is carried out when Ti atoms react either with N_2 or CH_4 providing the formation of TiN or TiC coatings. The multilayer architecture constituted by alternating layers of TiC and TiN were obtained by changing the (N_2 + Ar) and (CH_4 + Ar) reactive gases in the plasma atmosphere.

Plasma nitriding was carried out at 520ºC, for 2 hours, in a 95% H_2 + 5% N_2 atmosphere. The 100 nm thick titanium interlayer was deposited during 2 minutes. PVD coatings were performed at 300ºC under - 40 VDC bias, 640W being applied to the cathode; pressure was maintained at 1×10^{-6} Torr and argon partial pressure was 3.0 mTorr. PVD coatings thickness varied from 2.0 to 2.7 µm. Part of the specimens were PVD coated without being plasma nitrided previously. Table 1 shows the nitriding and coating times and thicknesses of the ceramic layers deposited under 7 different coating conditions. The TiN*(A3) and TiC*(B3) films were obtained by depositing TiN and TiC onto a non-nitrided H13 substrate. TiN(A3), TiC(B3) and TiC(B2) specimens were duplex coated, the ceramic layers being deposited onto pre-nitride H13 tool steel.. The Multilayer-w/o-Nit specimen was coated with a multilayer deposited onto the quenched and tempered H13 steel. The Multilayer-w-Nit specimen was duplex treated, the multilayer coating being deposited over a plasma nitrided substrate.

Table 1. Nitriding and coating times and thicknesses of the ceramic layers deposited under seven different coating conditions

Specimen	t_{nit}(h)	Film	t_{dep}(h)	t (µm)
TiN*(A3)	0	TiN	3,2	2,0
TiC*(B3)	0	TiC	3,0	2,1
TiN(A3)	2	TiN	3,0	2,3
TiC (B3)	2	TiC	4,0	2,2
TiC (B2)	2	TiC	2,0	2,4
Multilayer-w/o-Nit	0	TiC(B2)-TiN(A3)-TiC(B3)	4,6	2,7
Multilayer-w-Nit	2	TiC(B2)-TiN(A3)-TiC(B3)	4,6	2,7

The coatings were chemically and structurally characterized by X Ray Diffraction, WDX, Raman and XPS Spectroscopy after being deposited over Si wafers. Mechanical and Tribological properties were assessed via depth sensing and micro-scratch techniques applied to coatings deposited onto the H13 quenched and tempered tool steel.

Structural and Chemical Characterization

Ti + N_2 Reactive Deposition

Figure 1 shows X-ray diffractograms of coatings obtained under four different conditions of (Ti + N_2) reactive deposition A1, A2, A3 and A4. Nitrogen atomic contents, measured using WDS techniques are also shown. In addition, the metallic Ti diffractogram is also shown for comparison purposes.
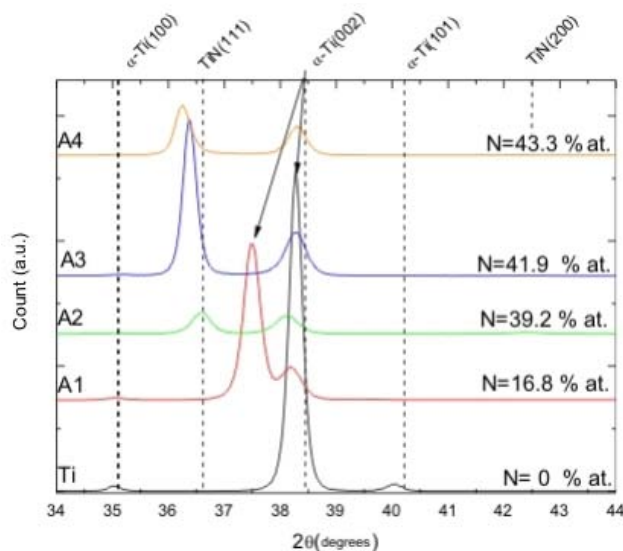
Figure 1. X-ray diffractograms of 4 different films obtained under different conditions of (Ti + N_2) reactive deposition A1, A2, A3 and A4. The N_2 content in the sputtering gas increases from A1 to A4.

The (α-Ti) peak shows up in all diffractograms, as the metallic Ti interlayer deposited prior to the reactive sputtering is detected.

Increasing the nitrogen flux and nitrogen partial pressure, during deposition, leads to greater nitrogen contents in the film. When the nitrogen over argon flux ratio $F_{reactive}/F_{Ar}$ increases from to 0.05 to 0.1 the nitrogen content changes from 16.8 at.% to 39.2 at.%. Nevertheless, increasing the $F_{reactive}/F_{Ar}$ ratio from 0.1 to 0.4 leads to a very low change of the nitrogen content from 39.2 at.% to 43.3 at.%.

The maximum nitrogen equilibrium content in (α-Ti) at 300ºC calculated using Thermocalc is approximately 10 at.%. The sputtering process is typically a non-equilibrium one and supersaturated metastable (α-Ti) with 16.8 at% N in solution is obtained. The α-Ti (002) peak is shifted to the left due to nitrogen supersaturation at the octahedral sites of the hexagonal unit cell.

TiN with a cF8 NaCl unit cell forms for the A2, A3 and A4 conditions. The film texture changed for the A3 deposition, the (111) orientation turning out to be very strong.

Ti + CH4 Reactive deposition

The increase of the methane flux and methane partial pressure for the *Ti + CH4* reactive deposition leads to greater carbon contents (measured by XPS) in the film as shown in Figure 2.

18th IFHTSE CONGRESS
International Federation for Heat Treatment and Surface Engineering

IFHTSE

ANAIS
PROCEEDINGS
ISSN 1516-392X
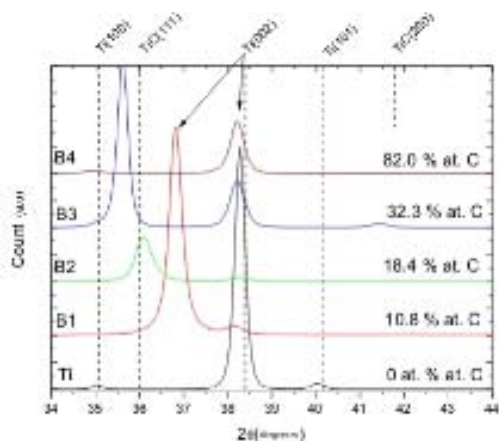
Figure 2. X-ray diffractogram of 4 different films obtained under different conditions of (Ti + CH$_4$) reactive deposition B1, B2, B3 and B4. The CH$_4$ content in the sputtering gas increases from B1 to B4.

The maximum solubility of carbon in (α-Ti) at 300ºC is 0.07 at.% according Thermocalc. The (Ti + CH$_4$) reactive deposition using the B1 condition leads to the formation of supersaturated hexagonal (α-Ti) containing 10.8 at.% of carbon. For the B2 and B3 conditions 18.4 at.% and 32.3 at.% of carbon are dissolved in the cF8 NaCl type TiC phase, respectively. A slight shift of the (111) plane for lower 2θ values can be attributed to changes in chemical composition and stress states of the TiC films.[1] The B3 condition leads to a buildup of a strong (111) texture.

For the B4 reactive deposition condition only α-Ti peaks were detected, originated in the Ti interlayer beneath. No TiC diffraction peaks were detected, probably due, to a very low TiC volume fraction and a very small crystallite size, of the order of nanometers. The B4 reactive deposition led to formation of a coating containing 81.9 at. % carbon.

Raman and XPS spectroscopy taken of the B4 film are shown in Figures 3 e 4.
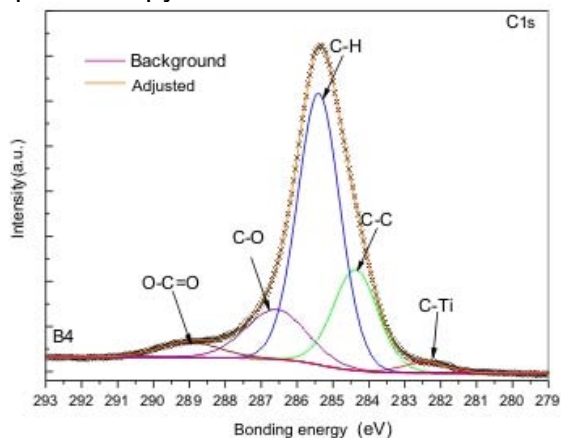
Figure 3. XPS spectroscopy of the TiC/a-C:H film obtained in the B4 condition.
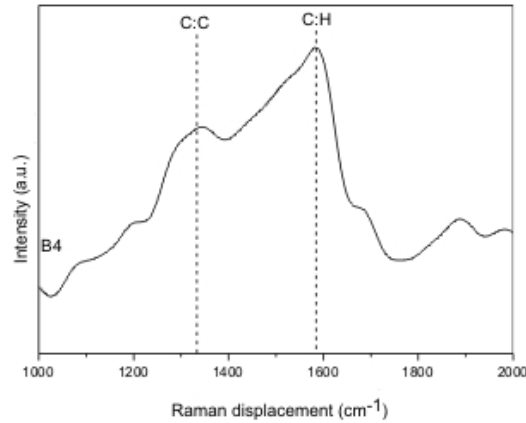
Figure 4. Raman spectroscopy of the B4 coating, using a 514,5 nm laser wavelength.

O-C=O e C-O structures indicate the presence of surface oxide layers, 3-4 nm thick. aC:H phase was detected both by XPS and Raman spectroscopy. In the Raman spectrum two asymmetric peaks were observed, the first one at 1345 cm^{-1}, known as G (Grafitic, sp^2), indicating graphitic distorted planes. A second one at 1580 cm^{-1}, known as D (Disorder, sp^2-sp^3) is usually attributed to disorder created by sp^3 bonding in the aC:H phase.

C-H structures with a 284.6 eV bonding energy and C-Ti with a 281.8 eV bonding energy were observed in the XPS spectrum, indicating the formation of a mixture of amorphous plus crystalline phases in the B4 film. Most probably an amorphous hydrogenated carbon phase matrix containing very small crystals of TiC was formed.

Figure 5 shows that increasing the methane content in the reactive gas increases the Ti-C/Ti ratio from 0.14 to 0.27, 0.43, and 0.49 for the B1, B2, B3 and B4 conditions and shifts X-ray diffraction peaks to the left, indicating that more carbon atoms occupy octahedral interstice sites of the TiC unit cell, as shown in Figure 2.
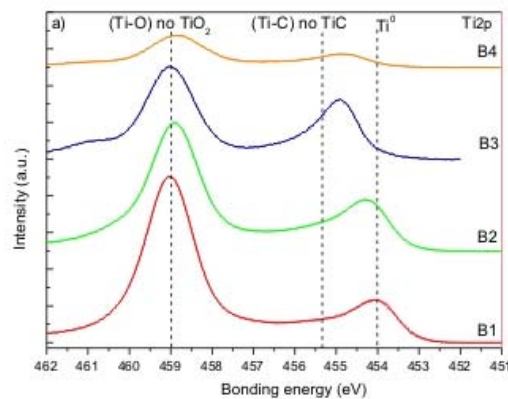
Figure 5. Ti2p XPS spectra of different films obtained for B1, B2, B3 and B4 conditions and increasing methane contents um the gas.

The ratio of TiC to the amorphous aC:H phase, not taking in account the presence of oxygen, was calculated and found to be 0.11 for the B4 condition. For the other three conditions no formation of hydrogenated carbon amorphous phase was detected. The formation of the aC:H amorphous phase is favored by greater amounts of methane in the reactive gas, probably due to a more intense target poisoning effect of the CHx species.

1.1 Adhesion of monolayer and multilayer films deposited onto H13 tool steel

Adhesion of the films to the substrate was assessed using the Rockwell C and micro-scratch adhesion tests.

1.1.1 Monolayer films

Table 2 summarizes the mechanical properties, measured by depth-sensing techniques, of the monolayer films deposited onto non-nitrided and pre-nitrided quenched and tempered H13 tool steel. TiN(A3) and TiN(B3) films show hardness around 30 GPa and Young modulus around 280 GPa, although the B3 film deposited onto the pre-nitrided specimen showed a Young modulus a little bit lower (260 GPa).

Table 2. Mechanical properties of monolayer films deposited onto non-nitrided and pre-nitrided quenched and tempered H13 tool steel

Specimen	H(GPa)	E(GPa).	Film	t (µm)
TiN*(A3)	28,6 ± 1,6	283,8 ± 8,5	TiN	2,0
TiC*(B3)	33,7 ± 1,4	259,9 ± 5,0	TiC	2,1
TiN(A3)	30,6 ± 1,2	280,3 ± 6,8	TiN	2,3
TiC (B3)	28,6 ± 1,6	283,8 ± 8,5	TiC	2,2
TiC (B2)	17,9 ± 0,7	193,0 ± 4,8	TiC	2,4

* stands for TiN coating deposited onto non-nitrided H13 specimens

Hardness and Young modulus of the non-nitrided and pre-nitrided quenched and tempered H13 tool steel were also measured obtaining H_{H13}= 7,2 ± 0,9 GPa and Y_{H13} = 202 ± 4,7 GPa, respectively and hardness on top of the nitrided layer and Young modulus on top of the nitrided H13 tool steel H_{NIT} = 14,3 ± 0,4 GPa and H_{NIT} = 220 ± 3,6 GPa, respectively.

Table 3 shows the results of Rockwell C and micro-scratch adhesion tests. The quality indexes HF of the surface around the indentation, for the TiN*(A3) and TiC*(B3), deposited onto non-nitrided quenched and tempered H13 were poor namely HF4 and HF5. The TiN(A3), TiC(B3) and TiC(B2) coatings deposited onto the plasma pre-nitrided specimens showed a very good quality index HF1. The results obtained in the Rockwell C adhesion tests show the significant role the plasma nitrided layer plays by increasing the load bearing capacity of the substrate.[4,5] Nevertheless, this technique, cannot differentiate the adhesion of the monolayer films TiN(A3), TiC(B2) and TiC(B3) deposited onto the pre-nitrided steel. The Rockwell C adhesion test is strongly dependent on the substrate hardness and film thickness as discussed by Ollendor.[3]

The critical loads for formation of the first cracks in the ceramic films (L_{c1}) and for delamination of the film (L_{c2}) in the scratch test, corresponding, respectively to cohesive and adhesive failures, are also shown in Table 3. Once again, one can see that the non-nitrided specimens show very low $L_{c1 \text{ and }}$ L_{c2} critical loads while for the pre-nitrided specimens the critical loads are much greater. It is worth noting that the TiC*(B3) coating, deposited onto the non-nitride H13 steel, showed a high quality index HF1 but did not behave in the same manner during the scratch test, the Lc1 and Lc2 critical loads being smaller than the ones obtained for the duplex treated specimens.

Table 3. Rockwell C and scratch test adhesion tests of monolayer films deposited onto non-nitrided and pre-nitrided quenched and tempered H13 tool steel

Specimen	HF	L_{C1} (N)	L_{C2} (N)
TiN*(A3)	4	4,5 ± 0,5	15,3 ± 2,4
TiC*(B3)	5	2,7 ± 2,0	8,4 ± 2,2
TiN(A3)	1	36,4 ± 2,1	54,0 ± 4,8
TiC(B3)	1	5,8 ± 2,4	11,6 ± 1,6
TiC(B2)	1	13,9 ± 1,0	24,1 ± 2,3

stands for TiN coating deposited onto non-nitrided H13 specimens

Table 4 shows the elastic recovery (W_e), and the resistance to elastic (H/E*) and plastic (H^3/E^{*2}) deformation of the ceramic films, obtained in the indentation tests.

Table 4. Critical loads, elastic recovery, H/E* and H^3/E^{*2} ratios for the ceramic films and the H13 tool steel

Specimen	LC1 (N)	LC2 (N)	w_e(%)	H/E*x10-2	H^3/E^{*2}(GPa)
TiN(A3)	36.4 ± 2.1	54.0 ± 4.8	59 ± 2	10.9 ± 0.5	0.36 ± 0.05
TiC(B2)	13.9 ± 1.0	24.1 ± 2.3	57 ± 2	9.3 ± 0.4	0.15 ± 0.05
TiN*(A3)	4.5 ± 0.5	15.3 ± 2.4	55 ± 2	10.0 ± 0.4	0.29 ± 0.06
TiC(B3)	5.8 ± 2.4	11.6 ± 1.6	77 ± 1	13.3 ± 0.4	0.68 ± 0.06
TiC*(B3)	2.7 ± 2.0	8.4 ± 2.2	80 ± 1	13.0 ± 0.3	0.57 ± 0.08
H13 pre-nitrided	-------	-------	43 ± 2	6.5 ± 0.2	0.06 ± 0.01
H13 non-nitrided	-------	-------	24 ± 3	3.5 ± 0.3	0.03 ± 0.01

The TiN(A3) and TiC(B2) ceramic films, deposited onto the nitrided H13 steel specimens, show the same elastic recovery (57%) and H/E* ratios (0.1), although their resistance to plastic deformation (H^3/E^{*2}) are quite different.

The TiC(B2) and the substrate undergo elastic-plastic deformation and the adhesive failure is mainly determined by the low resistance of the TiC(B2) film to plastic deformation.

When comparing films with different H^3/E^{*2} ratios and quite same elastic recoveries (58%) and H/E* ratios, deposited onto substrates with similar elastic-plastic properties, one can see that increasing the resistance to plastic deformation (H^3/E^{*2}) of the film increases the adhesion of the film to the substrate, as seen for the TiN(A3) film deposited onto pre-nitrided H13 steel. Besides the effect of the increase in the load bearing capacity of the substrate, the increase in the resistance to plastic deformation of the film plays an important role for improving the adhesion.

The TiN(A3) and TiN*(A3) films show the same elastic recoveries, same H/E* ratios and same resistance to plastic deformation (H^3/E^{*2}). In this case only the greater load bearing capacity of the substrate was decisive to increase the adhesion. The observed loss of adhesion can be attributed to an egg shell effect as proposed by Nix.[2] The same behavior was observed for the TiC(B3) e TiC*(B3) films deposited onto nitrided and non-nitrided H13 substrates, respectively.

No improvement of adhesion of the TiC(B3) film, deposited onto pre-nitrided H13 specimens, was observed, despite the greater load bearing capacity of the nitrided substrate. In this case the determining factor of this behavior is the great difference

between the elastic-plastic properties of the film and the substrate. The increase in hardness granted by the plasma nitriding treatment was not sufficient to reach hardness values near 34 GPa, as reported in Table 2, for the TiC(B3) film.

Plasma nitriding of the H13 substrate appears to be useful to increase the adhesion of deposited TiN films. On the other hand, the nitriding treatment did not show any beneficial effect on the adhesion properties of TiC ceramic films.

Adhesion of the multi-layer coating onto H13 tool steel

Based on the supposition that a more gentle transition of elastic-plastic properties of the layers in the film can improve the adhesion to the substrate, an attempt was made to obtain a functionally graded multi-layer film, with smaller differences of elastic-plastic properties. The H/E^* and H^3/E^{*2} ratios and the elastic recovery were gradually increased, by choosing an appropriate sequence of deposition and corresponding deposition processes.

The 2.7 µm thick multilayer film is composed initially by a 100 nm thick metallic Ti interlayer to improve adhesion, followed by a TiC(B2) layer with 0.6 µm and then by a 0.8 µm thick TiN(A3) layer. The outermost layer 1.0 µm thick is a TiC(B3) film. Figure 6 shows the structure of the multi-layer film deposited onto the nitrided H13 tool steel.
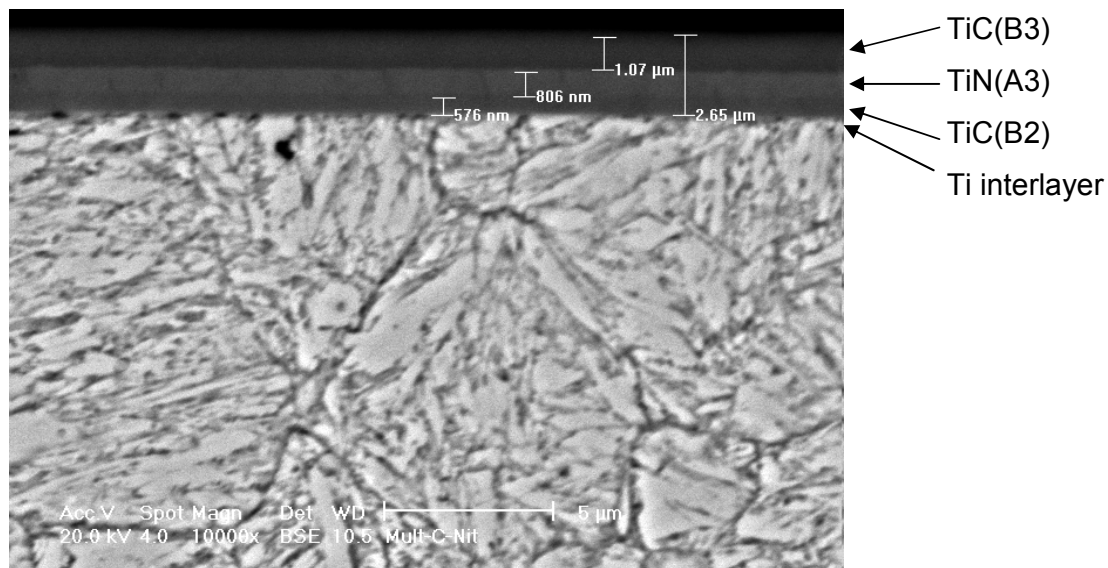
Figure 6. SEM image of the multi-layer film deposited onto pre-nitrided AISI H13 steel.

Table 5 shows the results of the Rockwell C and micro-scratch adhesion tests for the multilayer films. The result for the TiN*(A3) is also shown for comparison purposes.

Table 5. Rockwell C and micro-scratch adhesion tests for multi-layer films deposited onto non-nitride and pre-nitrided H13 tool steel substrates

Specimen	HF	L_{C1} (N)	L_{C2} (N)
Multi-layer-w/o-Nit	1	6,9 ± 2,3	16,7 ± 1,4
Multi-layer-w-Nit	1	8,8 ± 0,5	28,8 ± 4,4
TiN*(A3)	4	4,5 ± 0,5	15,3 ± 2,4

The critical load for cohesive failure of the multi-layer coatings did not show any significant increase over the critical loads observed for the TiN(A3) condition. The increase of the load bearing capacity of the substrate did not have any significant influence over the Lc1 critical load for cohesive failure. A cohesive failure characterized by delamination of the TiC(B3), TiN(A3) and/or TiC(B2) layers was observed as shown in Figure 7.

Plasma nitriding had an evident beneficial effect on the L_{c2} critical load for adhesive failure The multi-layer film deposited onto the nitrided H133 steel showed the same L_{c2} value shown by the TiC(B2) deposited onto the same substrate. Despite this result, the gradual change of elastic-plastic properties of the multi-layer films, did not yield greater Lc critical loads for failure when compared to the TiN(A3) monolayer film deposited onto nitrided H13 specimens.

These results point out the important role the outermost layer TiC(B2), with its low H^3/E^{*2} ratio, plays in increasing the adhesion to the substrate. The critical loads observed in this case were very similar to those obtained for the monolayer film TiC(B2).
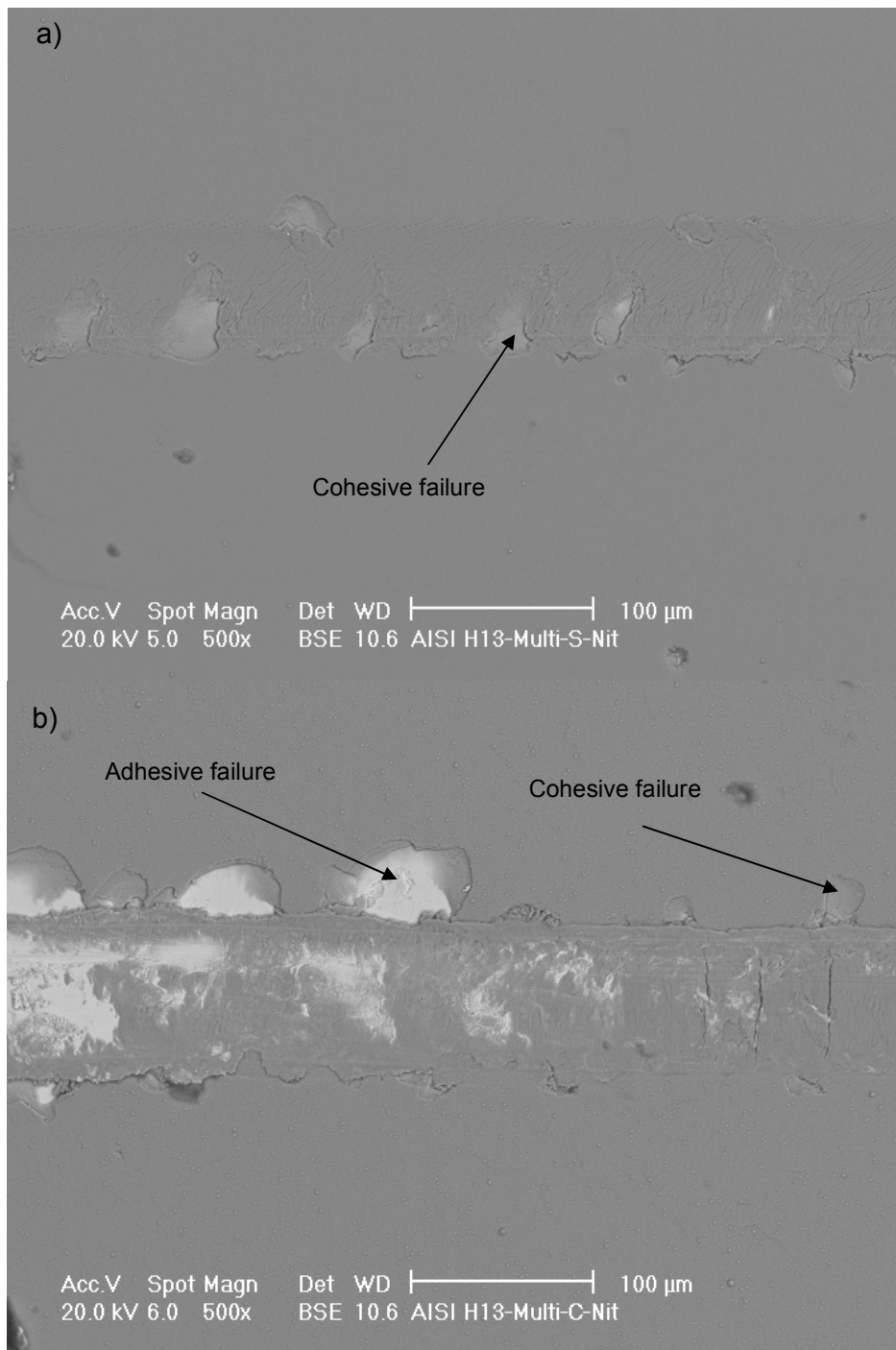
Figure 7. Multi-layer coatings (a) Cohesive failure of the coating deposited onto non-nitrided H13 tool steel; (b) Adhesive and cohesive failure of the multi-layer coating deposited onto nitrided H13 toll steel. Scratch test performed from the right to left.

CONCLUSIONS

DC magnetron sputtering allowed obtaining nitrogen or carbon supersaturated α-Ti, TiN, TiC or aC:H/TiC nanocomposite. Nitrogen or carbon supersaturated α-Ti films were obtained using low reactive gas fluxes in the sputtering gas. The ac:H/TiC nanocomposite was obtained using high methane flux in the sputtering gas.

B4 and B3 films showed an interesting combination of mechanical properties with high hardness (15 GPa), low reduced Young moduli (140 GPa) and high elastic recoveries (74%), derived from microstructures composed by a combination of amorphous and nanocrystalline phases present in the microstructure.

Different metallic, ceramic and composite films were obtained with hardness varying from 11 GPa to 38 GPa, reduced Young moduli from 138 GPa to a 295 GPa, H/E^* ratios from 0.067 to 0.133, H^3/E^{*2} ratios from 0.048 GPa to 0.67 GPa and elastic recovery varying from 43 to 77 %.

A functionally graded coating with a smooth variation of mechanical properties could be obtained by depositing an engineered sequence of Ti_N and TiC films onto nitrided and non-nitrided H13 tool steel specimens.

The adhesion tests showed that the adhesion of the film to the substrate is very low for films deposited onto non-nitrided H13 tool steel, the quality index, obtained in the Rockwell C test, being HF4 and HF6.

The duplex treatment grants a good adhesion of TiN films to the pre-nitrided substrate, increasing the critical load for cracking and delamination.

The duplex treatment does not assure a good adhesion of TiC ceramic films due to great differences of mechanical properties between the film and the substrate.

The Rockwell C adhesion test could not be used to rank the adhesion behavior of multi-layer films deposited onto non-nitrided and pre-nitrided H13 steel. Both showed a quality index HF1.

The TiC(B2) film and the multi-layer coating showed similar L_{C2} critical loads, 24 N and 28 N, respectively. The low resistance of the outermost TiC(B2) film to plastic deformation led to similar values of for the L_{C2} critical loads in the two coatings.

Acknowledgements

REFERENCES

1   Inoue, S. Wada, Y. Koterazawa, K. Deposition of TiC films by dual source dc magnetron sputtering. Vacuum, v. 59, p.735-741, 2000.
2   Nix, W. D.; A.K. Bhattacharya. Analysis of elastic and plastic deformation associated with indentation testing of thin film on substrates. Int. J. Solid Structures, v.24, p. 1287-1298, 1988.
3   Ollendor, H. Schneider D. A comparative study of adhesion test methods for hard coatings. Surface and Coatings Technology, v.113, p.86-102, 1999.
4   Sun, Y.; Bloyce, A.; Bell,T. Finite element analysis of plastic deformation of various TiN coating/ substrate systems under normal contact with a rigid sphere,Thin Solid Films, v. 271, p.122-131,1995.
5   Recco, A.A.C.; Oliveira, I.C.; Massi, M.; Maciel, H.S.; Tschiptschin,A.P. Adhesion of reactive magnetron sputtered TINx and TICy coatings to AISI H13 tool steel, Surface and Coatings Technology, v. 202, p. 1078-1083, 2007.